



Circulating PD-L1 is associated with T cell infiltration and predicts prognosis in patients with CRLM following hepatic resection

Xiuxing Chen^{1,2,3} · Ziming Du^{1,4,5} · Mayan Huang^{1,6} · Deshen Wang^{1,2} · William Pat Fong^{1,2} · Jieying Liang^{1,2} · Lei Fan⁷ · Yun Wang^{1,8} · Hui Yang^{1,2} · Zhigang Chen^{1,2} · Mingtao Hu^{1,2} · Ruihua Xu^{1,2} · Yuhong Li^{1,2} 

Received: 7 March 2021 / Accepted: 20 July 2021 / Published online: 28 July 2021
© The Author(s), under exclusive licence to Springer-Verlag GmbH Germany, part of Springer Nature 2021

Abstract

Background Exosomal PD-L1 (exoPD-L1) could induce immunosuppression functionally, thus impairing patients' survival in melanoma, NSCLC, and gastric cancer. However, no evidence demonstrates the feasibility of circulating exoPD-L1 and soluble PD-L1 (sPD-L1) as biomarkers for prognosis and early recurrence in colorectal liver metastasis (CRLM) patients following hepatectomy or their association with T cell infiltration at liver metastases.

Methods In cohort 1, exoPD-L1 and sPD-L1 were preoperatively tested using ELISA. CD3, CD8, granzyme B (GB) and PD1 expressed at liver metastases were evaluated using immunohistochemistry. In cohort 2, exoPD-L1 and sPD-L1 were detected at baseline, before hepatectomy, after hepatectomy, and after disease progression.

Results In cohort 1, higher preoperative exoPD-L1 or sPD-L1 significantly impaired RFS (exoPD-L1, $P = 0.0043$; sPD-L1, $P = 0.0041$) and OS (exoPD-L1, $P = 0.0034$; sPD-L1, $P = 0.0061$). Furthermore, preoperative exoPD-L1 was negatively correlated with CD3 + T-lymphocytes infiltrated at tumor center (CT), and GB and PD1 were expressed at tumor invasive margin (IM). Preoperative sPD-L1 was negatively correlated with CD3 + and CD8 + T-lymphocytes' infiltration at IM and CT, GB and PD1 expression at IM. In cohort 2, exoPD-L1 and sPD-L1 levels decreased following hepatectomy but increased when tumor progressed. Moreover, higher postoperative exoPD-L1 and sPD-L1 or a small reduction in exoPD-L1 and sPD-L1 levels after hepatectomy suggested higher early recurrence rate.

Conclusions Both preoperative exoPD-L1 and sPD-L1 had promising prognostic values and were associated with T cell infiltration at liver metastases in CRLM patients following hepatectomy. Dynamically tracking exoPD-L1 and sPD-L1 levels could monitor disease status and detect early recurrence.

Keywords Exosomal PD-L1 · Soluble PD-L1 · T cell infiltration · Colorectal liver metastasis · Hepatectomy · Prognosis

Introduction

Colorectal cancer is the third most common malignancy and the second leading cause of cancer-related death in the world [1]. Approximately 50% of CRC patients will develop liver metastases during the course of their disease [2]. Liver metastasectomy remains the most important treatment

strategy of acquiring long-term survival for colorectal cancer patients with only liver metastases (CRLM), with overall survival rates of 40% and 25% at 5 and 10 years, respectively [3]. Nevertheless, not all patients could benefit from hepatic metastasectomy with as much as 60% of patients suffering from recurrence, of which half are early relapses that subsequently greatly impair the overall survival rates [4]. Various scoring systems utilizing clinical variables have been proposed to predict the postoperative prognosis of CRLM patients, among which Fong et al.'s clinical risk score (CRS) system is the most commonly used [5]. However, the survival rate may differ even among patients with the same CRS score, which warrants finding more precise predictive biomarkers able to detect early recurrence and assist in clinical decision making.

Xiuxing Chen, Ziming Du and Mayan Huang have contributed equally.

✉ Ruihua Xu
xurh@sysucc.org.cn

✉ Yuhong Li
liyh@sysucc.org.cn

Extended author information available on the last page of the article

The immune microenvironment plays an important role in the occurrence and progression of CRLM. Previously, both Mlecnik et al.'s and our team's results have demonstrated that the immune score system, which is based on the densities of CD3 + and CD8 + immune cells in the center tumor (CT) and invasive margin (IM) regions in liver metastasis sites, can predict the prognosis after surgical resection [6, 7]. CRLM patients with a high immune score have prolonged overall survival than those with a low immune score [6]. Nonetheless, the immune score evaluation of liver metastases is only known after immunohistochemistry examination of a liver resection specimen, thus limiting the possibilities of pre-surgical decision. Moreover, the mechanisms of immune changes in patients with CRLM remain unclear.

Programmed death 1 ligand 1 (PD-L1) is widely expressed on various cell types, mainly in tumor cells, monocytes, macrophages, natural killer cells, dendritic cells, and activated T cells [8]. PD-L1 can interact with its receptor programmed cell death protein 1 (PD-1), transmitting a negative signal to control a series of processes of T cell-mediated cellular immune responses [9, 10]. Studies have reported that both tumor cells and immunocytes can release extracellular or soluble PD-L1 (sPD-L1) to peripheral circulation [11]. In human blood, there are three main forms of sPD-L1, including exosomal PD-L1 (exoPD-L1), microvesicles, and freely soluble forms of PD-L1, which include secreted variants or cleaved forms [9, 12, 13]. Exosomes are 30–150 nm biologically active lipid-bilayer nanovesicles secreted by various cell types composed of nucleic acids, lipids as well as proteins [14]. Microvesicles are larger vesicles (about 100–1000 nm), which are formed by budding directly from the plasma membrane [9]. Recently, emerging evidence has shown that the exosomes can carry PD-L1 in the same membrane topology as the cell surface and can contribute to suppress the anti-tumor immune response [15]. It has been proven that exosomes play a critical role in the formation of the tumor immune microenvironment [16]. Previous studies found that exoPD-L1 could be used as a prognostic biomarker in melanoma, non-small cell lung cancer (NSCLC), and gastric cancer [17–19]. However, the relationship between exoPD-L1 and T cell infiltration in liver metastasis and patients' prognosis in CRLM has not been reported yet.

Our study aims to elucidate whether exoPD-L1 and sPD-L1 correlate with T lymphocyte infiltration in liver metastases as well as to bring forward their use as not only potent prognosis biomarkers but also as follow-up biomarkers for monitoring disease status and predicting early recurrence in CRLM patients.

Method

Patient selection and follow-up

Patients pathologically diagnosed with CRLM at Sun Yat-sen University Cancer Center from January 1, 2005, to August 30, 2019, were enrolled in this study. The eligibility criteria were as follows: 1. pathologically confirmed CRLM; 2. underwent resection of the primary tumor and liver metastases; 3. no extra-hepatic metastases; 4. without other types of cancer. Treatment plans of CRLM patients were decided by the oncologists in our institution. In general, for CRLM patients who were initially resectable and with a low risk of recurrence (CRS 0–2), surgery of metastasis and/or primary sites was recommended; for CRLM patients who were initially unresectable or technically resectable but with over five metastasis lesions or a high risk of recurrence (CRS 3–5), preoperative chemotherapy would be considered. During the chemotherapy, the multidisciplinary team (MDT) would discuss the necessity and feasibility of surgery. After surgery, postoperative chemotherapy was recommended routinely. After 3–4 weeks of hepatectomy, patients would start postoperative surveillance every three months in the first 2 years and then every 6–12 months for up to a total of 5 years. After 5 years, the patients were followed up once a year. Cohort 1 consisted of patients who underwent curative hepatic resection, blood samples were collected within a month prior to hepatectomy, and post-surgery liver specimens were accessible. Cohort 2 consisted of blood samples collected at the beginning of treatment or within a month prior to hepatectomy or following hepatectomy or after disease progression. We followed the patients up to April 30, 2020, by contacting the patients or informed relatives.

Exosomes and microvesicles extraction

A total of 200 µl plasma samples were collected from each CRLM patient for exosomes isolation using ExoQuick™ Exosome Precipitation Solution (SBI, USA) according to the manufacturer's instructions. Briefly, plasma samples were centrifuged at $2,000 \times g$ for 30 min to remove cells and debris. Then, plasma samples were thawed, and thrombin was added at room temperature for 5 min following centrifuging at 10,000 rpm for 5 min to collect clear plasma. The supernatant was then centrifuged at $16,500 \times g$ for 30 min to obtain microvesicles [20]. 50.4 µl exosome precipitation solution reagent was then added, and the mixture was incubated at 4 °C for 30 min and further centrifuged at $1500 \times g$ for 30 min to obtain the exosomes. Afterward, the supernatant was collected to detect free-form sPD-L1 expression.

Exosome and microvesicle identification

We used Western blotting to test the expression of exosomal markers [CD9 (1: 1000, Proteintech, USA), CD63 (1: 1000, Proteintech, USA), TSG101 (1: 1000, Proteintech, USA)] and microvesicular markers [CD63 (1: 1000, Proteintech, USA), TSG101 (1: 1000, Proteintech, USA), Actinin-4 (1:1000, Proteintech, USA) and Annexin A1 (1:1000, Proteintech, USA)] of isolated exosomes and microvesicles. Actinin-4 and Annexin A1 markers were used to distinguish isolated microvesicles from exosomes. We used JEM-1400 transmission electron microscope (TEM, JEOL, Japan) to photograph isolated exosomes and microvesicles to assess their size and shape. We used NS300 Instrument (NanoSight, UK) with Nanoparticle Tracking Analysis (NTA) software to determine the size and concentration of exosomes and microvesicles.

Determination of PD-L1 concentration in plasma and circulating exosomes

sPD-L1, exoPD-L1, microvesicular PD-L1 and free-form sPD-L1 concentration were measured using Human PD-L1/B7-H1 Valukine™ ELISA kit (R&D, USA) according to manufacturer's instructions. sPD-L1 was detected using plasma without centrifugation. Samples and standards were measured in duplicate.

Immunohistochemistry

Immunohistochemistry was performed using the standardized streptavidin-peroxidase method. The 4- μ m thickness paraffin-embedded human tissue microarray sections were deparaffinized and rehydrated, followed by heat-induced antigen retrieval. Then, the slides were incubated with antibodies specific for CD3 (1:100, ZSGS-BIO, China), CD8 (1:100, ZSGS-BIO, China), granzyme B (1:50, GB, ZSGS-BIO, China), PD1 (1:50, ZSGS-BIO, China) overnight at 4 °C. The slides were incubated with biotinylated goat anti-rabbit IgG for 1 h at 37 °C, followed by incubation with peroxidase-conjugated streptavidin for 30 min at room temperature for detection. The visualization was performed using 3,3'-diaminobenzidine (DAB, Dako, Denmark) according to the manufacturer's instructions. Immunostaining of each marker on tissue samples was assessed by a pathologist. The densities of CD3+ and CD8+ T cells in both the tumor center (CT) and invasive margin (IM) regions were obtained as previously described [6]. PD1 and GB expression were determined as a percentage of PD1- or GB-positive cells over total mononuclear cells and counted in 5 high-power fields (HPF, \times 200) in the IM.

Endpoints

Relapse-free survival (RFS) was defined as the time from liver resection to the evidence of relapse or metastasis to other organs or death, whichever occurred first. Overall survival (OS) was defined as the time from liver resection to death from any cause. Postoperative response was defined as response after the postoperative treatment period assessed using response evaluation criteria in solid tumors (RECIST 1.1). Resection status was defined as no evidence of disease (NED) or not (non-NED) after therapy. Those with evidence of tumor by imaging combined with serum CEA level examination were considered to be in a non-NED state, otherwise were defined as NED. Early recurrence was defined as the presence of metastases in the liver or other organs after liver metastasectomy within 6 months.

Statistical analysis

Statistical analysis was performed using GraphPad prism software (version 5.01), IBM SPSS Statistics software (version 22.0), and R studio software (Version 1.2.1335). Error bars shown in graphical data represent medians and interquartile range (IQR). Spearman correlation coefficients were calculated to identify the relationship of continuous data between groups. The correlation of sPD-L1 or exoPD-L1 with clinicopathological characteristics was examined using Kendall's tau-b correlation test. The cutoffs for the sPD-L1 or exoPD-L1 were determined using maximally selected rank statistics in R [21]. Survival data were analyzed using Kaplan–Meier survival curve (tested by log-rank test) and Cox proportional hazards model. Cox proportional hazards models' results were presented as hazard ratios (HRs) with 95% confidence interval (95% CI). A two-tailed value of $p < 0.05$ was determined as statistically significant.

Results

Patients

To analyze whether circulating PD-L1 could act as potential biomarkers and its correlation with immune infiltration of tumors, we ultimately enrolled 177 patients in cohort 1, including 120 men and 57 women with a median age of 57 (range 20–83) years. Eighty-nine (50.28%) patients received preoperative chemotherapy, while 88 (49.72%) did not. The clinicopathologic characteristics of patients enrolled in cohort 1 are summarized in Table 1.

Cohort 2 was designed to monitor how the level of preoperative circulating PD-L1 associates with the disease status of CRLM patients and to analyze how postoperative circulating PD-L1 correlates with early recurrence.

Table 1 Basic clinicopathological characteristics of patients in cohort 1

Variables	Total patients		
	No. of patients (%)	<i>P</i> values* (exoPD-L1)	<i>P</i> values* (sPD-L1)
Age			
> =65	39 (22.03)	0.873	0.544
<65	138 (77.97)		
Gender			
Male	120 (67.80)	0.254	0.596
Female	57 (32.20)		
Pathological grade			
G1–2	137 (77.40)	0.112	0.003
G3	40 (22.60)		
Histological subtype			
Non-mucinous	172 (97.18)	0.633	0.541
Mucinous	5 (2.82)		
Primary tumor T stage			
Tis-3	117(66.10)	0.709	0.032
T4	47(26.55)		
Missing	13(7.35)		
Primary tumor N stage			
N0	62 (35.03)	0.030	0.087
N1-2	107 (60.45)		
Missing	8 (4.52)		
Primary tumor site			
Right-sided	35 (19.77)	0.896	0.543
Left-sided	142 (80.23)		
Primary tumor size		0.873	0.708
≤ 5 cm	83 (46.89)		
> 5 cm	25 (14.12)		
Missing	69 (38.98)		
Vascular invasion		0.051	0.008
No	97(54.80)		
Yes	27(15.30)		
Missing	53(29.94)		
Nerve invasion		0.981	0.802
No	85(48.02)		
Yes	39(22.03)		
Missing	53(29.95)		
Preoperative CEA		0.044	0.066
≤200 ng/ml	167 (94.35)		
> 200 ng/ml	10 (5.65)		
Interval from primary tumor resection to liver metastases	0.197		
≤ 12 months	146 (82.49)		
> 12 months	31 (17.51)		
Number of metastases per patient		0.994	0.433
≤ 1	76 (42.94)		
> 1	101 (57.06)		
Size of the largest metastasis		0.009	0.013
≤ 5 cm	154 (87.01)		
> 5 cm	23 (12.99)		
Resection type of liver metastasis and primary tumor		0.994	0.125
Simultaneous resection	90 (50.8)		

Table 1 (continued)

Variables	Total patients		
	No. of patients (%)	<i>P</i> values* (exoPD-L1)	<i>P</i> values* (sPD-L1)
Staged resection	87 (40.2)		
Preoperative chemotherapy		0.326	0.088
No	88(49.72)		
Yes	89 (50.28)		
Chemotherapy	60 (33.90)		
Cetuximab-based	17 (9.60)		
Bevacizumab-based	12 (6.78)		
Postoperative chemotherapy		0.996	0.766
No	46 (25.99)		
Yes	131 (74.01)		
Chemotherapy	109(61.58)		
Cetuximab-based	14 (7.91)		
Bevacizumab-based	8 (4.52)		
Ablation		0.974	0.774
No	153(86.40)		
Yes	24(13.60)		
CRS		0.021	0.057
0–2	102 (57.63)		
3–5	67 (47.85)		
Missing	8 (4.52)		
KRAS		0.063	0.065
Wild-type	61 (34.46)		
Mutation-type	22 (12.43)		
Missing	94 (53.11)		

*Correlation between basic clinicopathological characteristics and exoPD-L1 or Spd-11 using Kendall's tau-b correlation test

Four time points were set: beginning of treatment (baseline, 23 patients), before metastasectomy (preoperation, 49 patients), after metastasectomy (postoperation, 46 patients), and following disease progression (progression, 16 patients). Five patients whose blood samples had been collected in all 4 time points in this cohort. Among the 49 patients enrolled, 38 were males and 11 were females, with a median age at diagnosis of 54 (range 20–83) years with a median follow-up of 14.8 months. Twenty-two patients (44.9%) in cohort 2 underwent resection of primary tumor and liver metastases concurrently. Twenty-seven patients (55.1%) had primary tumor resection before liver metastasectomy, and their blood samples were collected before liver resection. The clinicopathologic characteristics and treatment information of patients enrolled in cohort 2 are detailed in Supplementary Table 2. A flow chart representing patient selection is shown in supplementary Fig. 1.

ExoPD-L1 strongly correlates with sPD-L1 expression level

In order to explore different forms of sPD-L1 expression level, we isolated the exosomes and microvesicles, as well as freely soluble forms of PD-L1 from the plasma of 10 CRLM patients. We used TEM and NTA and western blot analysis to verify the morphology, size, and purity of isolated exosomes (Fig. 1A–C) and microvesicles (supplementary Fig. 2A–C). The median level of sPD-L1 was 567.00 pg/mL ($n = 10$). The level of exoPD-L1 ($n = 10$, median 222.67 pg/mL) was significantly higher compared to microvesicular PD-L1 ($n = 10$, median 135.49 pg/mL) and free-form sPD-L1 ($n = 10$, median 129.21 pg/mL) in the plasma (Fig. 1D). ExoPD-L1 showed a strong correlation with sPD-L1, while microvesicle and other freely soluble forms of PD-L1 did not, which would suggest that exoPD-L1 is the most dominant component of sPD-L1

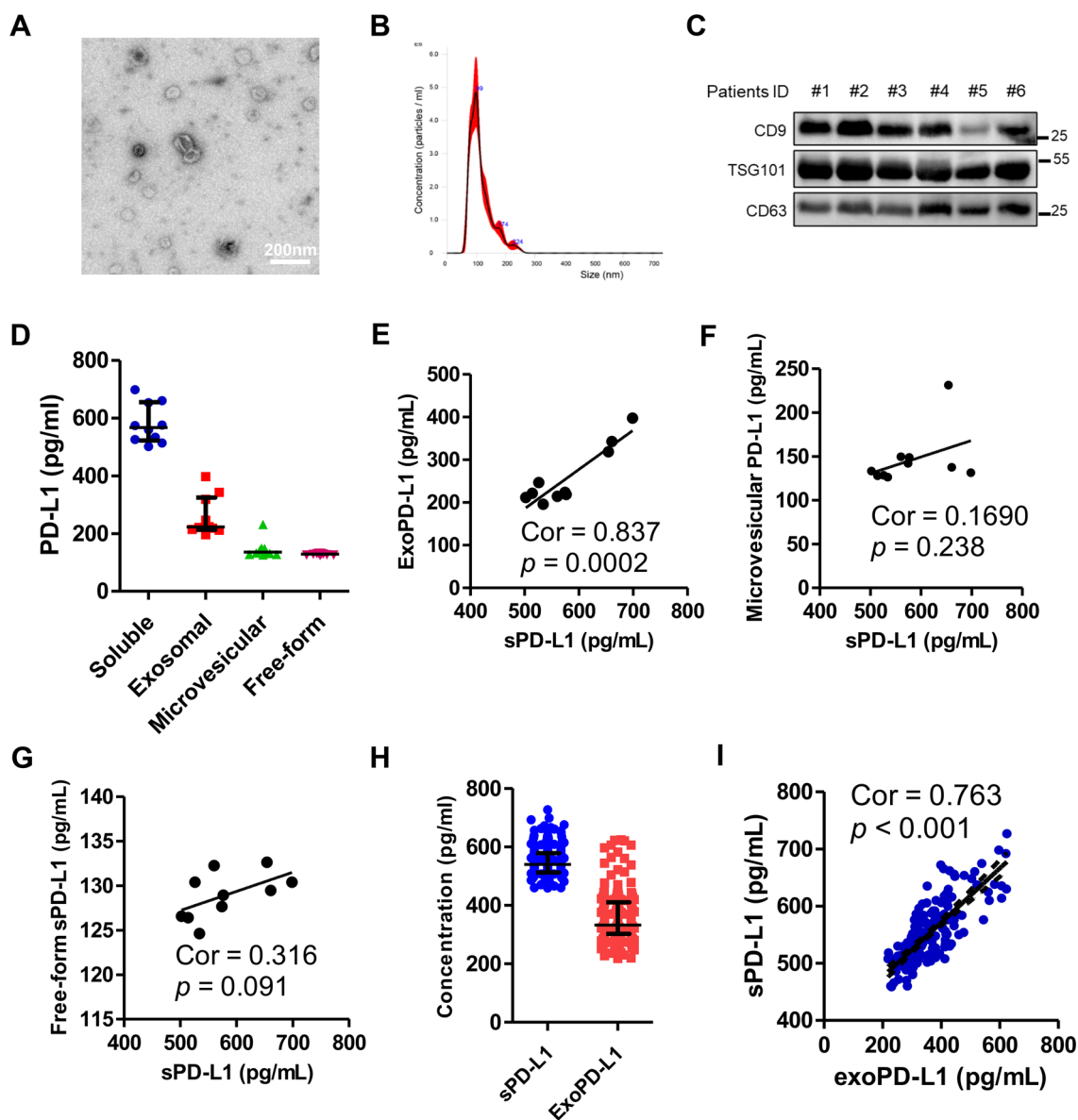


Fig. 1 Isolated exosome characterization and the correlation between exoPD-L1 and sPD-L1. **A** A representative TEM image of purified exosomes from patients' plasma. Scale bar, 200 nm. **B** Characterization of purified exosomes using nanoparticle tracking. **C** Representative immunoblots showing expression of CD9, TSG101 and CD63 in plasma exosomes derived from six patients. **D** Different PD-L1 expression levels of multiple forms isolated from ten patients.

E Strong correlation between preoperative sPD-L1 and exoPD-L1 ($P=0.002$, $r=0.837$, $n=10$). No correlation between preoperative **F** sPD-L1 and **G** microvesicular PD-L1 ($P=0.238$, $n=10$) and free-form sPD-L1 ($P=0.091$, $n=10$). **H** Expression levels of sPD-L1 and exoPD-L1 isolated from 177 patients in cohort 1. **I** Strong correlation between preoperative exoPD-L1 and sPD-L1 in cohort 1 (Spearman's correlation at $P<0.001$, $r=0.763$, $n=177$)

(Fig. 1E–F). We then detected the expression level of sPD-L1 and exoPD-L1 in patients of cohort 1. Overall, the median level of sPD-L1 and exoPD-L1 was 539.99 pg/mL ($n=177$) and 221.33 pg/mL ($n=177$), respectively (Fig. 1H). ExoPD-L1 showed a high degree of association with sPD-L1 with a correlation index of 0.763 ($p<0.001$, $n=177$), which is in accordance with the previous results obtained from the 10 patients (Fig. 1I).

Association of preoperative circulating PD-L1 expression with clinical variables

ExoPD-L1 and sPD-L1 expression detected from patients of cohort 1 showed that preoperative exoPD-L1 level was significantly associated with primary tumor N stage ($p=0.030$), preoperative CEA ($p=0.044$), size of the max metastases ($p=0.009$) and CRS ($p=0.021$), while preoperative

sPD-L1 level was significantly associated with pathological grade ($p=0.003$), primary tumor T stage ($p=0.032$), vascular invasion ($p=0.008$), and size of the largest metastases ($p=0.013$) (Table 1). Preoperative exoPD-L1 level ($p=0.326$) and preoperative sPD-L1 level ($p=0.088$) were similar between patients with or without preoperative chemotherapy.

Prognostic role of preoperative circulating PD-L1 in CRLM

According to exoPD-L1 and sPD-L1 levels in cohort 1, cut-off values of 244.00 pg/mL and 551.82 pg/mL defined by maximally selected rank statistics in R were used for survival analysis. In univariate analysis, either exoPD-L1 or

sPD-L1 showed a strong negative correlation with RFS (exoPD-L1, $P=0.0043$; sPD-L1, $P=0.0041$) and OS (exoPD-L1, $P=0.0034$; sPD-L1, $P=0.0061$) as shown in Fig. 2 and Table 2. In multivariate Cox proportional hazards model analysis, both exoPD-L1 and sPD-L1 high levels were correlated with poor RFS (exoPD-L1: HR 1.555, 95% CI 1.033–2.342, $P=0.035$; sPD-L1: HR 1.555, 95% CI 1.033–2.341, $P=0.034$) and OS (exoPD-L1: HR 2.120, 95%CI 1.160–3.874, $P=0.015$;sPD-L1: HR 2.19; 95% CI 1.197–4.112; $P=0.011$) independently (Table 2 and supplementary Table 1).

We further investigated the prognostic value of a risk score combining the CRS and sPD-L1 or exoPD-L1. Prognostic value was improved as the AUC at 1-year RFS prediction increased (combination group vs. CRS group

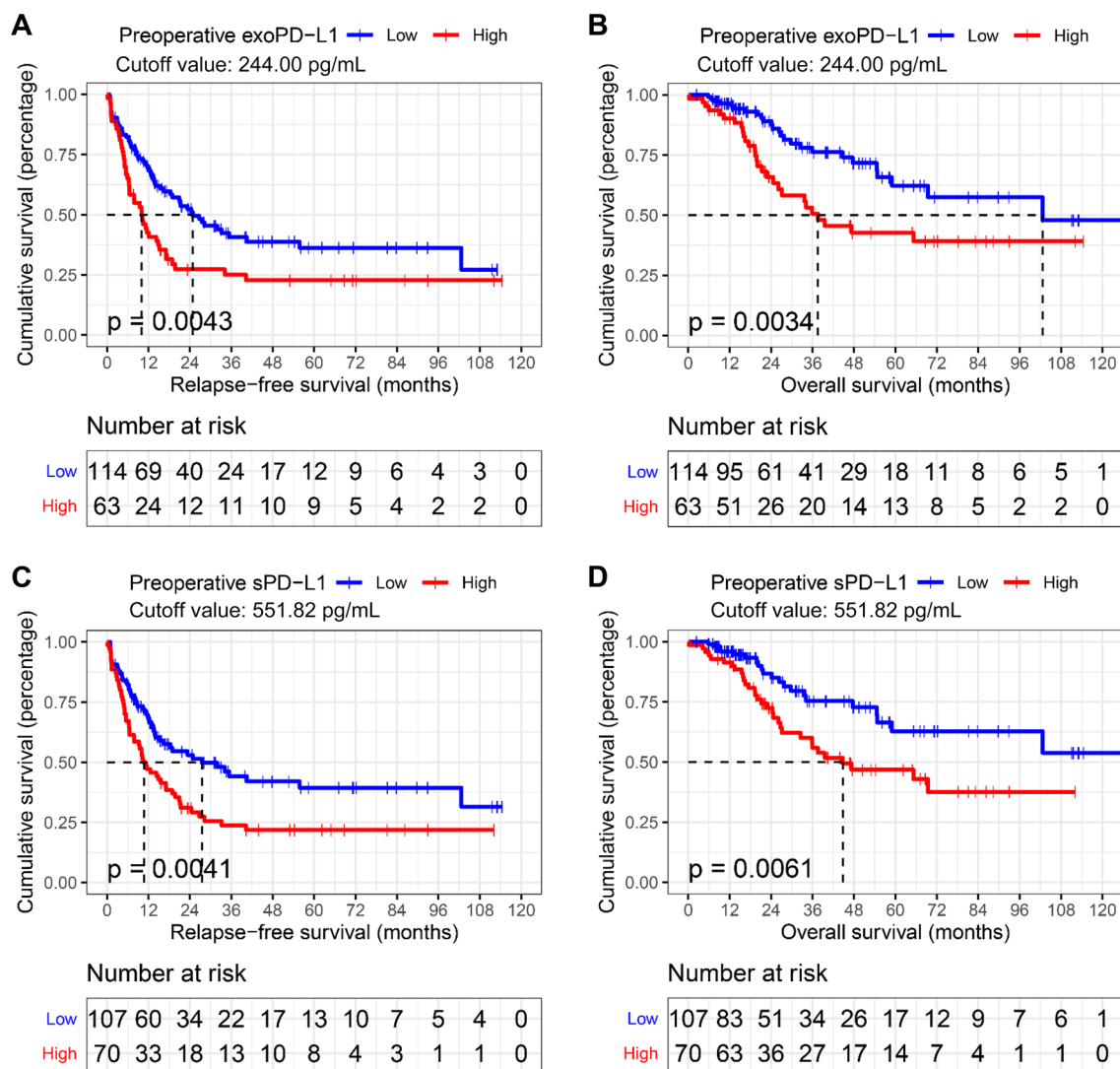


Fig. 2 Both preoperative exoPD-L1 and sPD-L can be used as biomarkers of survival. Kaplan–Meier estimation of **A** relapse-free survival ($p=0.0043$) and **B** overall survival ($p=0.0034$) in patients

according to preoperative exoPD-L1 levels; Kaplan–Meier estimation of **C** relapse-free survival ($p=0.0041$) and **D** overall survival ($p=0.0061$) in patients according to preoperative sPD-L1

Table 2 Univariate and multivariate analysis results of clinicopathological characteristics and preoperative sPD-L1 as well as exoPD-L1

Variables	Relapse-free survival				Overall survival			
	Univariate analysis		Multivariate analysis		Univariate analysis		Multivariate analysis	
	HR (95% CI)	<i>P</i> value	HR (95% CI)	<i>P</i> value	HR (95% CI)	<i>P</i> value	HR (95% CI)	<i>P</i> value
Age (> 65 vs. ≤ 65)	0.905(0.561–1.460)	0.682			1.582(0.857–2.918)	0.142		
Gender (Female vs. male)	1.009(0.673–1.514)	0.966			0.918(0.524–1.606)	0.763		
Primary tumor site (Right-sided vs. Left-sided)	0.919(0.574–1.473)	0.727			0.925(0.463–1.844)	0.824		
Tumor grade (G3 vs. G1–2)	1.805(1.180–2.762)	0.007	1.909(1.208–3.018)	0.006	1.474(0.810–2.681)	0.204		
Pathological type (Mucinous vs. Non-mucinous)	3.094(0.965–9.925)	0.058			0.53(0.073–3.856)	0.531		
T-stage (T4 vs. Tis-3)	1.101(0.720–1.684)	0.657			1.853(1.044–3.291)	0.035	1.747(1.040–2.936)	0.035
N-stage (N1–2 vs. N0)	1.898(1.227–2.936)	0.004	1.668(1.069–2.604)	0.024	2.291(1.211–4.335)	0.011		
Preoperative CEA (> 200 vs. ≤ 200 ng/ml)	1.584(0.694–3.616)	0.275			3.087(1.316–7.243)	0.010		
Interval from primary tumor resection to liver metastases (≤ 12 vs. > 12 months)	1.208(0.742–1.968)	0.448			1.689(0.902–3.163)	0.102		
Number of metastases (> 1 vs. ≤ 1)	1.954(1.305–2.924)	0.001			1.262(0.730–2.183)	0.405		
Size of the largest metastasis (> 5 cm vs. ≤ 5 cm)	2.359(1.395–3.989)	0.001	2.314(1.310–4.089)	0.004	4.54(2.402–8.583)	< 0.001	3.622(1.719–7.631)	0.001
Preoperative chemotherapy (Yes vs. no)	2.146(1.435–3.208)	< 0.001	2.449(1.596–3.758)	< 0.001	1.400(0.804–2.438)	0.234		
Postoperative chemotherapy (Yes vs. no)	0.846(0.551–1.298)	0.444			0.449(0.257–0.784)	0.005		
Ablation (Yes vs. no)	1.723(1.003–2.961)	0.049			1.461(0.617–3.46)	0.388		
Exosomal PD-L1 (High vs. low)	1.747(1.184–2.576)	0.005	1.555(1.033–2.342)	0.035	2.197(1.280–3.772)	0.004	2.120(1.160–3.874)	0.015
Soluble PD-L1 (High vs. low)	1.823(1.242–2.676)	0.002			2.133(1.225–3.714)	0.007		

vs. exoPD-L1 group: 0.713 vs. 0.664 vs. 0.625; combination group vs. CRS group vs. sPD-L1 group: 0.691 vs. 0.664 vs. 0.591) and at 3-year OS prediction increased (combination group vs. CRS group vs. exoPD-L1 group: 0.698 vs. 0.642 vs. 0.617; combination group vs. CRS group vs. sPD-L1 group: 0.691 vs. 0.642 vs. 0.585), as presented in Supplementary Fig. 3A–D. Next, we evaluated the prognostic value of the exoPD-L1 and sPD-L1 among patients with the same CRS. Among the 177 CRLM patients, 102 (57.63%) had a low CRS (0–2), 67 (47.85%) had a high CRS (3–5), whereas 8 (4.52%) were missing. In the low CRS group, patients with low exoPD-L1 obtained a higher median RFS (40.5 vs. 15.2 months;

$P = 0.044$; Supplementary Fig. 3E) but failed to have a higher median OS (103 vs. not reached months; $P = 0.37$; Supplementary Fig. 3F) than those with high exoPD-L1. Patients with low sPD-L1 had both a higher median RFS (55.8 vs. 19.8 months; $P = 0.038$; Supplementary Fig. 3G) and a higher median OS (not reached vs. 69.4 months; $P = 0.0084$; Supplementary Fig. 3H) than those with high sPD-L1. In the high CRS group, patients with low exoPD-L1 obtained a higher median OS (not reached vs. 22.7 months; $P = 0.0037$; Supplementary Fig. 3I) and tended to have a higher median RFS (11.76 vs. 6.47 months; $P = 0.092$; Supplementary Fig. 3I) than those with high exoPD-L1. SPD-L1 failed to distinguish RFS and OS in the high CRS group.

Circulating PD-L1 correlates with T lymphocytes infiltration and activation as well as PD1 expression at liver metastasis sites

We then used IHC to detect the expression levels of T lymphocyte infiltration markers (CD3, CD8) and activation marker (GB) coupled with PD1 in liver metastasis with the aim of analyzing their association with circulating PD-L1 level (Supplementary Fig. 3). As shown in Fig. 3A–F, higher level exoPD-L1 showed a significant negative correlation to CD3 + T lymphocytes infiltrated at CT (Spearman's correlation at $P=0.027$, $r=-0.172$), GB ($P<0.001$, $r=-0.331$) and PD1 ($P=0.008$, $r=-0.212$) expressed at IM. Interestingly, sPD-L1 was significantly negatively related to CD3 + T lymphocytes infiltrated at both tumor CT ($P=0.003$, $r=-0.228$), and IM ($P<0.001$, $r=-0.270$), and CD8 + T lymphocytes infiltrated at CT ($P=0.046$, $r=-0.155$), and IM ($P=0.001$, $r=-0.256$), sPD-L1 also showed a notable negative relation to GB ($P=0.002$, $r=-0.261$) and PD1 ($P=0.003$, $r=-0.236$) expression at IM (Fig. 3G–L).

To this date, there have been no studies on the prognostic value of GB and PD1 expressed at liver metastasis of CRLM patients. We thus proceeded by classifying patients with a GB expression above 8% or a PD1 expression above 40% into GB high expression group and PD1 high expression group, respectively. We found that patients in the high GB expression group had better RFS [median (95% CI): 31.9 months (18.4–45.5) vs. 12.3 months (6.3–18.2), $p=0.023$] and OS [median (95% CI): 102.6 months (69.4-not reached) vs. 37.5 months (14.5–60.6), $p=0.026$] than those in low group (Supplementary Fig. 5A–B). Patients in high PD1 expression group are presented with longer OS [median (95% CI): not reached vs. 54.6 months (40.6–68.6), $p=0.024$] than those with low expression (Supplementary Fig. 5D). However, RFS of patients showed no statistical difference between high and low PD1 expression groups [median (95% CI): 18.9 months (0–39.4) vs. 17.1 months (10.9–23.2), $p=0.68$, Supplementary Fig. 5C].

Dynamic changes in circulating PD-L1 level associates with CRLM disease status and early recurrence

Results obtained from patients in cohort 2 showed that exoPD-L1 level decreased significantly after both preoperative chemotherapy ($p<0.05$) and liver metastasectomy ($p<0.001$) but notably increased when tumor progressed ($p<0.05$) (Fig. 4A). As for sPD-L1, it distinctly decreased after liver surgery ($p<0.001$) but increased when tumor progression occurred ($p<0.05$) (Fig. 4B). Furthermore, sPD-L1 and exoPD-L1 levels of patients with postoperative NED status were significantly lower than patients who were

not ($p<0.001$) (Fig. 4C–D). Cutoff values of 109.03 pg/mL, 183.62 pg/mL, 60.08 pg/mL, and 338.71 pg/mL defined by maximally selected rank statistics in R were used for RFS analysis regarding postoperative exoPD-L1, postoperative sPD-L1, changes of exoPD-L1 and sPD-L1 before and after hepatectomy, respectively. Patients demonstrated higher early recurrence rate with higher-level postoperative exoPD-L1 (69.2% vs 12.1%, $p<0.001$) and higher-level sPD-L1 (52.9% vs 13.8%, $p=0.007$) (Fig. 4E). Patients who had higher decrease of exoPD-L1 (22.0% vs 80.0%, $p=0.018$) and sPD-L1 (14.8% vs 50.0%, $p=0.011$) before and after hepatectomy exhibited lower early recurrence rate (Fig. 4E). The AUCs to predict early recurrence were 0.720 (95% CI: 0.515–0.925, $P=0.022$) of postoperative exoPD-L1, 0.791 (95% CI: 0.629–0.962, $P=0.002$) of postoperative sPD-L1 and 0.692 (95% CI: 0.531–0.892, $P=0.028$) of changes of sPD-L1 before and after hepatectomy (Fig. 4F). However, the AUCs for changes of exoPD-L1 before and after hepatectomy (0.615, 95% CI: 0.413–0.808), postoperative CEA (0.609, 95% CI: 0.419–0.746) and changes of CEA before and after hepatectomy (0.507, 95% CI: 0.293–0.670) were not significant (Fig. 4F). Furthermore, higher postoperative level of exoPD-L1 [median (95% CI): 4.34 (1.15-not reached) vs. 15.18 (11.37-not reached), $p=0.0041$] and sPD-L1 [median (95% CI): 5.87 (4.04-not reached) vs. 15.54 (11.37-not reached), $p=0.0041$] suggested poorer RFS, while the higher decrease of exoPD-L1 [median (95% CI): 14.85 (9.26-not reached) vs. 1.15 (1.05-not reached), $p=0.0075$] and sPD-L1 [median (95% CI): 15.18 (10.38-not reached) vs. 5.87 (3.32-not reached), $p=0.052$] after liver surgery exhibited better RFS (Fig. 4G–J).

We have five patients whose blood samples had been collected in all 4 time points in cohort 2, and we analyzed the dynamic changes of circulating PD-L1 level through paired samples. The first three patients experienced no early recurrence while the last two experienced. In general, our results showed that exoPD-L1 and sPD-L1 decreased as tumor response detected in the scan after preoperative chemotherapy and further decreased after curative hepatic resection and increased as tumor relapse or progress detected in the scan (Supplementary Fig. 6A–E).

Discussion

Our results show a strong correlation between exoPD-L1 and sPD-L1 levels in CRLM patients. In cohort 1, we demonstrated that both preoperative exoPD-L1 and sPD-L1 had effective prognostic values in CRLM patients undergoing liver metastasectomy, even in patients with similar CRS score. Furthermore, we are first to report that high levels of exoPD-L1 and sPD-L1 negatively correlate with T lymphocyte infiltration and activation in liver metastasis.

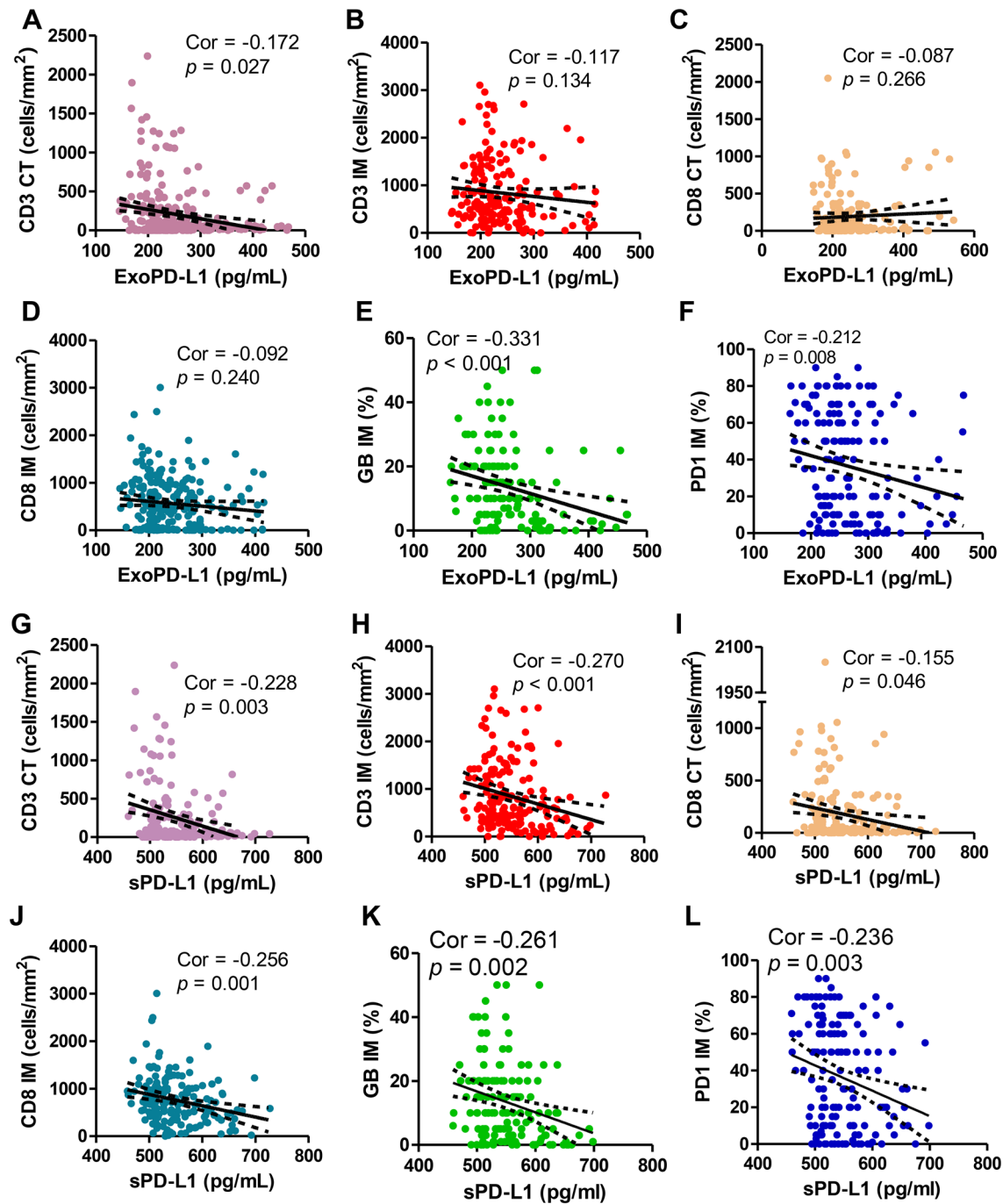


Fig. 3 Preoperative exoPD-L1 and sPD-L1 showed strong degree of correlation with activate immune status in colorectal liver metastasis sites. Preoperative exoPD-L1 showed high correlation with **A** CD3+T cell infiltration at the tumor center (CT) (Spearman's correlation at $P=0.027$, $r=-0.170$), **E** GB expression at the invasive margin (IM) ($P<0.001$, $r=-0.331$), and **F** PD1 expression at CT ($P=0.008$, $r=0.212$), but no correlation with **B** CD3+T cell infiltration in invasive at CT ($P=0.134$, $r=0.117$) and **C** CD8+T cell infiltration at CT ($P=0.266$, $r=-0.087$) and **D** CD8+T cell

infiltration at IM ($P=0.240$, $r=-0.092$); preoperative sPD-L1 showed high degree of correlation with **G** CD3+T cell infiltration at the tumor center (CT) (Spearman's correlation at $P=0.003$, $r=-0.228$), **H** CD3+T cell infiltration at the invasive margin (IM) ($P<0.001$, $r=-0.270$), **I** CD8+T cell infiltration at CT ($P=0.046$, $r=-0.155$), **J** CD8+T cell infiltration at IM ($P=0.001$, $r=-0.256$), and **K** GB expression at IM ($P=0.002$, $r=-0.261$), and **L** PD1 expression at IM ($P=0.003$, $r=-0.236$)

Additionally, results from cohort 2 showed that dynamic tracking of both exoPD-L1 and sPD-L1 might be useful to monitor disease status and serve as predictive biomarkers for early recurrence in CRLM patients following hepatectomy.

Recently, several publications have shown that exoPD-L1 can be used to predict poor clinical outcomes in cancer patients [18, 19], which is in agreement with its use in CRLM. However, how exoPD-L1 affects the survival of patients with CRLM remains to be clarified. Emerging evidence has proved that exosomes play a critical role in the formation of the tumor immune microenvironment [16]. ExoPD-L1 is well positioned to mediate PD-1 interaction and immunosuppression because these exosomes co-express PD-L1 on its surface and peptide-MHC molecules critical for T cell signaling conduction [9]. Lung cancer cell-derived ExoPD-L1 can inhibit Jurkat T cells producing interferon- γ in vitro [22]. Theodoraki et al. found PD-L1^{high} but not PD-L1^{low} exosomes could downregulate T cell activation marker CD69 expression on activated CD8 + T cells [18]. Chen et al. indicated exoPD-L1 can suppress the proliferation and cytotoxicity of CD8 + T cells and facilitate tumor growth [20]. Poggio et al. suggested that exoPD-L1 contributes to immunosuppression and promotes tumor progression in prostate and colorectal cancer mouse model [23]. All these results suggest that exoPD-L1 can suppress CD8 + T activation mechanistically. Previous studies have found that CRLM patients with higher densities of CD3 + and CD8 + T cell infiltration in liver metastases had longer OS and PFS after hepatectomy [6, 7, 24, 25]. Higher CD3 + and CD8 + T cell infiltration in liver metastases correlated with longer OS and PFS after hepatectomy [6, 7]. In our results, patients with higher GB expression (an activation marker of T cells) in liver metastases also had better RFS ($p=0.023$) and OS ($p=0.0260$) (Supplementary Fig. 5A–B). Furthermore, exoPD-L1 was significantly and negatively correlated to CD3 + T lymphocytes infiltration and GB expression in liver metastases. Therefore, we speculate that the suppression of CD8 + T cell activation in liver metastasis may be partly related to the exoPD-L1 secretion.

Several studies also showed that high sPD-L1 level was associated with poor prognosis in different types of cancer [26–31]. Functional experiments show that sPD-L1 in sera can inhibit T cell function in vitro [32]. However, these studies do not distinguish which form of sPDL1 mediates such immunosuppressive and prognostic effects. In human blood, there are three main forms of sPD-L1, including exosomal PD-L1 (exoPD-L1), microvesicles and freely soluble forms of PD-L1 which include secreted variants or cleaved forms [9, 12, 13]. A review published at Nature reviews Immunology proposed that exoPD-L1 may be a more potent immunosuppressant and biomarker than other forms of extracellular PD-L1 [9]. Cell-free sPD-L1 has also been associated with inhibiting lymphocytes in vitro and in vivo, but a relatively

high concentration is needed [31, 33]. However, the activity of free-form sPDL1 has not been directly compared with that of exoPD-L1. As for microvesicular PD-L1, there is no evidence proving its role in T lymphocyte inhibition. Our results show that exoPD-L1 is the most abundant form of sPD-L1 in the plasma (Fig. 1D), and a similar trend was also found in melanoma patients [20]. Moreover, we found that exoPD-L1 strongly correlates with sPD-L1 expression (Fig. 1E–G), while other forms did not. Therefore, we inferred that exoPD-L1 might significantly contribute to the prognostic ability and immunosuppressive role of sPD-L1.

PD-L1 is widely expressed in a variety of cell types. Therefore, tumor cells and immune cells can release exosomes containing PD-L1 [8, 23, 34, 35]. One study reported that a single cancer cell could release thousands of exosomes leading to an abundance of circulating exoPD-L1 [36]. Another study reported that the levels of human exoPD-L1 were positively correlated with tumor size in a human-derived tumor xenograft model [23]. In our cohort 1, higher expression of sPD-L1 and exoPD-L1 was related to more significant liver metastasis lesions. In cohort 2, sPD-L1 and exoPD-L1 expression decreased after liver metastasectomy or chemotherapy and increased when disease progressed [23]. sPD-L1 and exoPD-L1 expressions were higher in patients with postoperative non-NED status in cohort 2. These findings suggest that sPD-L1 and exoPD-L1 levels after the resection of CRLM liver metastases can reflect tumor burden and minimal residual lesions. Therefore, failure to resolving sPD-L1 and exoPD-L1 levels following resection could indicate the presence of micrometastatic disease elsewhere.

The receptor of PD-L1, PD-1, is similarly used as an exhausted T cell marker and is expressed on activated T cell surface. However, we found that both exoPD-L1 and sPD-L1 correlated negatively with PD-1 expression. Several studies show that the predictive role of PD-1 expression is different across various types of cancer [37–43]. As for colorectal cancer, one study containing 356 cases from the Cancer Genome Atlas (TCGA) database as primary cohort and 276 patients from their own institution as training cohort both demonstrated that higher expressions of PD-1 correlates with better prognosis [44], which is agreement with our result. Moreover, a significant positive correlation between PD-1 expression and GB expression in liver metastasis sites ($r=0.390$, $p<0.001$) was observed.

There were some limitations to our study. Firstly, a subset of patients lacking blood and tissue samples was excluded, resulting in a limited sample size in both cohort 1 and cohort 2. Secondly, the medical information of patients was collected retrospectively. Thirdly, preoperative chemotherapy might have impacted the PD-L1 levels and survival outcomes, affecting the preoperative PD-L1 levels and prognostic values. Lastly, we adopted a single T

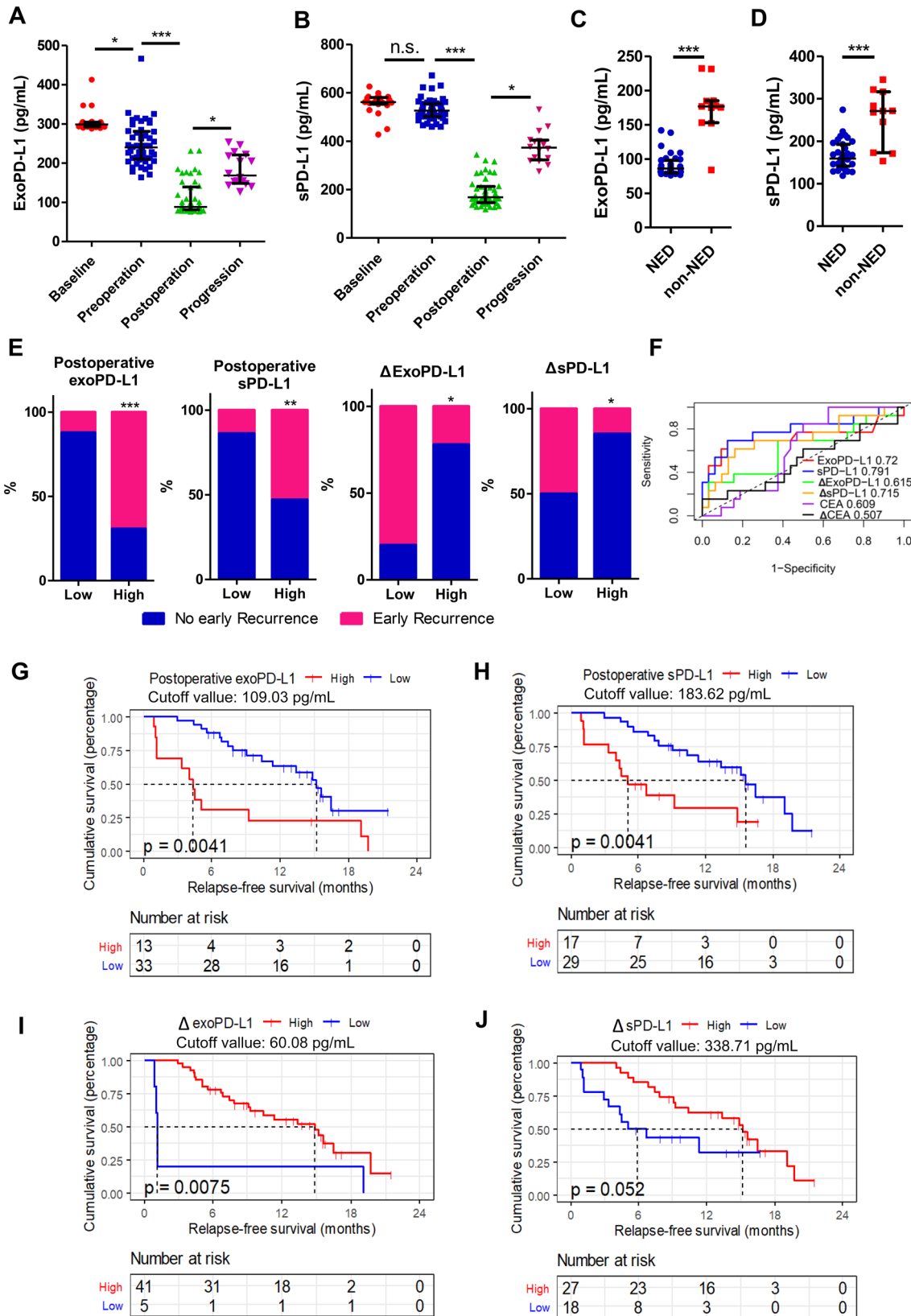


Fig. 4 Association between dynamic changes in circulating PD-L1 level and CRLM disease status as well as early recurrence. **A** Different sPD-L1 expression levels according to patients' disease status: sPD-L1 level is significantly higher at baseline and preoperatively and decreases postoperatively and increases when disease progressed; **B** different exoPD-L1 levels according to patients' disease status: exoPD-L1 level is highest at baseline and decreases preoperatively, there is a further reduction after surgery and an increment when disease progressed; **C** sPD-L1 is significantly higher in patients with non-NED status compared to NED status; **D** ExoPD-L1 is significantly higher at non-NED status compared with NED status; **E** early recurrence rate according to the different expression levels of postoperative exoPD-L1, postoperative sPD-L1 and expression level change of exoPD-L1 and sPD-L1 before and after hepatectomy; **F** ROC curves of postoperative exoPD-L1, sPD-L1, CEA or changes of exoPD-L1, sPD-L1 and CEA before and after hepatectomy to predict early recurrence; Kaplan–Meier estimation of relapse-free survival in patients according to **G** postoperative exoPD-L1 ($p=0.0041$); **H** postoperative sPD-L1 ($p=0.0041$); **I** changes of exoPD-L1 ($p=0.0075$) and **J** sPD-L1 ($p=0.052$) before and after hepatectomy. n.s., no significance; *, $P<0.05$; **, $P<0.01$; ***, $P<0.001$

lymphocyte activation marker (GB) in this study. Although this marker is mainly expressed on activated T cells, other lymphocytes such as natural killer cells and B cells [7] also express GB. Similarly, PD1 is also expressed on B cells, monocytes and MDSCs [40]. The use of flow cytometry, magnetic bead or multiple IHC to sort T lymphocytes and detect GB and PD1 expression could offer more precision and specificity in future studies.

In conclusion, both preoperative exoPD-L1 and sPD-L1 had promising prognostic values and correlated to T cell infiltration at liver metastases in CRLM patients following hepatectomy. Dynamically tracking exoPD-L1 and sPD-L1 levels could monitor disease status and detect early recurrence.

Supplementary Information The online version contains supplementary material available at <https://doi.org/10.1007/s00262-021-03021-3>.

Funding This work was supported by the National Natural Science Foundation of China (81872010).

Availability of data and material The authenticity of this article has been validated by uploading the key raw data onto the Research Data Deposit public platform (www.researchdata.org.cn).

Declarations

Conflicts of interest The authors declare that they do not have any conflict of interest.

Ethics approval All access to blood samples and clinical data for research was approved by the institutional review board and ethics committee of Sun Yat-sen University Cancer Center (B2020-018–01).

Consent to participate Written informed consent was provided by all participants of this study.

Consent for publication All authors reviewed and approved the manuscript for submission.

Reference:s

1. Bray F et al (2018) Global cancer statistics 2018: GLOBOCAN estimates of incidence and mortality worldwide for 36 cancers in 185 countries. *CA Cancer J Clin* 68(6):394–424
2. Dai Z et al (2012) Analysis and prediction of colorectal cancer incidence trend in China. *Zhonghua Yu Fang Yi Xue Za Zhi* 46(7):598–603
3. Abdalla EK et al (2004) Recurrence and outcomes following hepatic resection, radiofrequency ablation, and combined resection/ablation for colorectal liver metastases. *Ann Surg* 239(6):818–25
4. Iwai T et al (2020) Circulating cell-free long DNA fragments predict post-hepatectomy recurrence of colorectal liver metastases. *Eur J Surg Oncol* 46(1):108–114
5. Fong Y et al (1999) Clinical score for predicting recurrence after hepatic resection for metastatic colorectal cancer: analysis of 1001 consecutive cases. *Ann Surg* 230(3):309–18
6. Wang Y et al (2018) The Immunoscore system predicts prognosis after liver metastasectomy in colorectal cancer liver metastases. *Cancer Immunol Immunother* 67(3):435–444
7. Mlecnik B et al (2018) Comprehensive Intrametastatic Immune Quantification and Major Impact of Immunoscore on Survival. *J Natl Cancer Inst* 110(4):438
8. Francisco LM et al (2009) PD-L1 regulates the development, maintenance, and function of induced regulatory T cells. *J Exp Med* 206(13):3015–3029
9. Daassi D, Mahoney KM, Freeman GJ (2020) The importance of exosomal PDL1 in tumour immune evasion. *Nat Rev Immunol* 20(4):209–215
10. Xie F et al (2019) The role of exosomal PD-L1 in tumor progression and immunotherapy. *Mol Cancer* 18(1):146
11. Becker A et al (2016) Extracellular vesicles in cancer: cell-to-cell mediators of metastasis. *Cancer Cell* 30(6):836–848
12. Orme JJ et al (2020) ADAM10 and ADAM17 cleave PD-L1 to mediate PD-(L)1 inhibitor resistance. *Oncoimmunology* 9(1):1744980
13. Romero Y, Wise R, Zolkiewska A (2020) Proteolytic processing of PD-L1 by ADAM proteases in breast cancer cells. *Cancer Immunol Immunother* 69(1):43–55
14. Colombo M, Raposo G, Thery C (2014) Biogenesis, secretion, and intercellular interactions of exosomes and other extracellular vesicles. *Annu Rev Cell Dev Biol* 30:255–289
15. Morrissey SM, Yan J (2020) Exosomal PD-L1: Roles in Tumor Progression and Immunotherapy. *Trends Cancer* 6(7):550–558
16. Whiteside TL (2016) Exosomes and tumor-mediated immune suppression. *J Clin Invest* 126(4):1216–1223
17. Cordonnier M et al (2020) Tracking the evolution of circulating exosomal-PD-L1 to monitor melanoma patients. *J Extracell Vesicles* 9(1):1710899
18. Theodoraki MN et al (2018) Clinical significance of PD-L1(+) exosomes in plasma of head and neck cancer patients. *Clin Cancer Res* 24(4):896–905
19. Fan Y et al (2019) Exosomal PD-L1 retains immunosuppressive activity and is associated with gastric cancer prognosis. *Ann Surg Oncol* 26(11):3745–3755
20. Chen G et al (2018) Exosomal PD-L1 contributes to immunosuppression and is associated with anti-PD-1 response. *Nature* 560(7718):382–386

21. Wright MN, Dankowski T, Ziegler A (2017) Unbiased split variable selection for random survival forests using maximally selected rank statistics. *Stat Med* 36(8):1272–1284
22. Kim DH et al (2019) Exosomal PD-L1 promotes tumor growth through immune escape in non-small cell lung cancer. *Exp Mol Med* 51(8):1–13
23. Poggio M et al (2019) Suppression of exosomal PD-L1 induces systemic anti-tumor immunity and memory. *Cell* 177(2):414–427
24. Berthel A et al (2017) Detailed resolution analysis reveals spatial T cell heterogeneity in the invasive margin of colorectal cancer liver metastases associated with improved survival. *Oncoimmunology* 6(3):e1286436
25. Katz SC et al (2009) T cell infiltrate predicts long-term survival following resection of colorectal cancer liver metastases. *Ann Surg Oncol* 16(9):2524–2530
26. Chang B et al (2019) The correlation and prognostic value of serum levels of soluble programmed death protein 1 (sPD-1) and soluble programmed death-ligand 1 (sPD-L1) in patients with hepatocellular carcinoma. *Cancer Immunol Immunother* 68(3):353–363
27. Finkelmeier F et al (2016) High levels of the soluble programmed death-ligand (sPD-L1) identify hepatocellular carcinoma patients with a poor prognosis. *Eur J Cancer* 59:152–159
28. Kim HJ et al (2018) Clinical significance of soluble programmed cell death ligand-1 (sPD-L1) in hepatocellular carcinoma patients treated with radiotherapy. *Radiother Oncol* 129(1):130–135
29. Shigemori T et al (2018) Soluble PD-L1 Expression in Circulation as a Predictive Marker for Recurrence and Prognosis in Gastric Cancer: Direct Comparison of the Clinical Burden Between Tissue and Serum PD-L1 Expression. *Ann Surg Oncol* 26(3):876–883
30. Wei W et al (2018) Prognostic significance of circulating soluble programmed death ligand-1 in patients with solid tumors: A meta-analysis. *Medicine* 97(3):e9617
31. Yang KN et al (2019) Effects of different levels of soluble PD-L1 protein on the growth of Lewis lung cancer transplanted tumor. *J Biol Regul Homeost Agents* 33(2):537–542
32. Frigola X et al (2011) Identification of a soluble form of B7–H1 that retains immunosuppressive activity and is associated with aggressive renal cell carcinoma. *Clin Cancer Res* 17(7):1915–1923
33. Mahoney KM et al (2019) A secreted PD-L1 splice variant that covalently dimerizes and mediates immunosuppression. *Cancer Immunol Immunother* 68(3):421–432
34. Frigola X et al (2012) Soluble B7–H1: differences in production between dendritic cells and T cells. *Immunol Lett* 142(1–2):78–82
35. Ruffner MA et al (2009) B7–1/2, but not PD-L1/2 molecules, are required on IL-10-treated tolerogenic DC and DC-derived exosomes for in vivo function. *Eur J Immunol* 39(11):3084–3090
36. Alsaab HO et al (2017) PD-1 and PD-L1 checkpoint signaling inhibition for cancer immunotherapy: mechanism, combinations, and clinical outcome. *Front Pharmacol* 8:561
37. Owen D et al (2018) Expression patterns, prognostic value, and intratumoral heterogeneity of PD-L1 and PD-1 in thymoma and thymic carcinoma. *J Thorac Oncol* 13(8):1204–1212
38. Pollari M et al (2018) PD-L1(+) tumor-associated macrophages and PD-1(+) tumor-infiltrating lymphocytes predict survival in primary testicular lymphoma. *Haematologica* 103(11):1908–1914
39. Ren X et al (2018) PD1 protein expression in tumor infiltrated lymphocytes rather than PDL1 in tumor cells predicts survival in triple-negative breast cancer. *Cancer Biol Ther* 19(5):373–380
40. Kim JR et al (2013) Tumor infiltrating PD1-positive lymphocytes and the expression of PD-L1 predict poor prognosis of soft tissue sarcomas. *PLoS One* 8(12):e82870
41. Hohtari H et al (2019) Immune cell constitution in bone marrow microenvironment predicts outcome in adult ALL. *Leukemia* 33(7):1570–1582
42. Ma J et al (2019) PD1(Hi) CD8(+) T cells correlate with exhausted signature and poor clinical outcome in hepatocellular carcinoma. *J Immunother Cancer* 7(1):331
43. Ueda K et al (2018) Prognostic value of PD-1 and PD-L1 expression in patients with metastatic clear cell renal cell carcinoma. *Urol Oncol* 36(11):499.e9–499.e16
44. Li Y et al (2016) Prognostic impact of programmed cell death-1 (PD-1) and PD-ligand 1 (PD-L1) expression in cancer cells and tumor infiltrating lymphocytes in colorectal cancer. *Mol Cancer* 15(1):55

Publisher's Note Springer Nature remains neutral with regard to jurisdictional claims in published maps and institutional affiliations.

Authors and Affiliations

Xiuxing Chen^{1,2,3} · Ziming Du^{1,4,5} · Mayan Huang^{1,6} · Deshen Wang^{1,2} · William Pat Fong^{1,2} · Jieying Liang^{1,2} · Lei Fan⁷ · Yun Wang^{1,8} · Hui Yang^{1,2} · Zhigang Chen^{1,2} · Mingtao Hu^{1,2} · Ruihua Xu^{1,2} · Yuhong Li^{1,2} 

¹ State Key Laboratory of Oncology in South China and Collaborative Innovation Center for Cancer Medicine, Department of Medical Oncology, Sun Yat-Sen University Cancer Center, 651# Dongfeng Road East, Guangzhou 510060, People's Republic of China

² Department of Medical Oncology, Sun Yat-Sen University Cancer Center, Guangzhou, People's Republic of China

³ Department of Oncology, Sun Yat-Sen Memorial Hospital of Sun Yat-Sen University, Guangzhou, China

⁴ Guangdong Key Laboratory of Nasopharyngeal Carcinoma Diagnosis and Therapy, Guangzhou, People's Republic of China

⁵ Department of Molecular Diagnostics, Sun Yat-Sen University Cancer Center, Guangzhou, People's Republic of China

⁶ Department of Pathology, Sun Yat-Sen University Cancer Center, Guangzhou, People's Republic of China

⁷ School of Materials Science and Engineering and National Engineering Research Center for Tissue Restoration and Reconstruction, South China University of Technology, Guangzhou, People's Republic of China

⁸ Department of Hematologic Oncology, Sun Yat-Sen University Cancer Center, Guangzhou, People's Republic of China